S. Gisinger, J. Wagner, B. Witschas 14.07.2020

***Interactive comment on* "Airborne measurements and large-eddy simulations of small-scale Gravity Waves at the tropopause inversion layer over Scandinavia" *by* Sonja Gisinger et al.**

Authors' response to the comments of the anonymous Referee #1

We appreciate the positive feedback and the valuable comments of the two anonymous reviewers #1 and #2 which we considered carefully for our revision. Thus, changes in the content of the manuscript arose, especially with respect to the momentum flux (figures and discussion). These changes became necessary due to findings we made when incorporating the reviewers' comments. We spent some more time on the momentum flux calculations and the assessment of their sensitivity and uncertainty and managed to find a way of analyzing the momentum fluxes in measurements and simulations such that they provide robust vertical profiles in terms of their trend. The range of uncertainty for the quantitative momentum flux values is also included. Previously, we were not aware of the sensitivity of the averaged momentum flux, however, also thanks to the reviewer comments, we consider the sensitivity of the momentum flux calculation on the background removal and leg length in the revised momentum flux analysis and in the discussion of the manuscript. Below you will find a detailed explanation of the changes in the manuscript as well as the point-to-point answers to the review comments. All modified figures and one new figure are also attached at the end of this document.

Momentum flux

In the framework of the revision of the paper manuscript, we tried to quantify the influence of the reflected and trapped waves in the troposphere on the momentum flux (MF) profile (and also derived the MF profiles for the realistic simulation runs 5 and 6). By doing so, we realized that the determination of the perturbations u' and w' was not properly or rather not extensively enough described in the previous version of the manuscript. Moreover, during this analysis it turned out that the resulting MF profile is sensitive with respect to the background fit and the length and start/end points of the flight leg (not only for the measurements but also for the most idealized case of interfacial waves on a boundary layer inversion). By separating the leg into 3 segments for the measurements, we had already shown that there is a clear variability. But only after doing more detailed analyses and sensitivity test, we found out that we had drawn incomplete conclusions for the MF profile of the interfacial waves. The positive MF in the vicinity of the TIL is actually not due to the interfacial waves but due to the longer waves (>30 km) that are influenced by the TIL. The leg-averaged MF of the interfacial waves is close to zero (a detailed explanation is given below). The former downstream segment 3 was longer than segments 1 and 2, and thus, longer waves remained in u' and w' of segment 3. Considering this, we have carefully revised the parts of the manuscript that deal with the MF profiles.

The most important points/changes are:

+ We use spectral filters to determine u' and w' for different wave classes (long, intermediate, and short waves, i.e. mainly mountain waves, reflected and trapped waves in the troposphere, and interfacial waves). We separate the wave classes based on their horizontal wavelengths as seen in

the wavelet power spectra. long waves > 6 km and short waves < 6 km for the boundary layer simulations (Run 1, 2). Long waves > 30 km, intermediate waves 10 km to 30 km, and short waves < 10 km for the measurements and the TIL/no-TIL simulations (Run 5, 6). The advantage of the spectral filter is that the wavelengths contained in u' and w' are clearly defined. For the usual background fit, the wavelengths vary with the length of the leg. This is not appropriate for the purpose of our analyses. A similar separation of wave classes can be found in Georgelin and Lott 2001.

additional reference:

Georgelin, M. and Lott, F.: On the transfer of momentum by trapped lee waves: Case of the IOP 3 of PYREX, J. Atmos. Sci., 58, 3563–3580, https://doi.org/10.1175/1520-0469(2001)058<3563:OTTOMB>2.0.CO;2, 2001a.

+ Boundary layer simulations: we show the MF profile for the two wave classes in Fig. 13. When the MF is averaged for the whole domain, the MF profiles of the long waves and the short waves show a distinctive kink at the altitude of the inversion (Fig. 13e). This is not found when the inversion is absent (Fig. 13a). When the MF is averaged for the downstream region, the resulting MF of the interfacial waves depends on the exact start/end points of the downstream region with respect to the wave phase. This is because the interfacial waves show alternating positive and negative fluxes downstream of the mountain (Fig. 13b). In contrast to upward propagating mountain waves (Fig. 13d), the phase shift between u' and w' is -90° for interfacial below the inversion (Fig. 13c) and changes to +90° right above the inversion (not shown). When the MF is averaged over a downstream region that only contains full wave cycles, the resulting MF is zero for well-established and totally trapped interfacial waves (Fig. 13e). When the start/endpoints of the downstream region are chosen such that waves are partly included, the MF can be neg. (pos.) right below the inversion and pos. (neg.) above the inversion. The sign of the MF depends on the cutting location in the wave cycles, i.e. depends on if more neg. (pos.) MF is included in the average (Fig. 13b). This happened in Fig. 13 for the first version of the manuscript.

+Measurements and realistic simulations: A thousand sub-legs are created as such that their start (end) point is fixed at the westernmost (easternmost) point of the measurements and the length of the leg is stepwise extended eastward (westward) by 1 km starting with a minimum length of 200 km and going up to 700 km, i.e. the full leg length. This is done to incorporate the sensitivity of the leg-averaged MF with respect to the start/end points of the leg and the corresponding unequal sampling of updrafts and downdrafts as already suggested and analyzed in a similar way by Brown (1983). We additionally found differences in the MF from lidar and HALO in-situ data at 7.8 km altitude, although one hardly can determine differences in u and w between lidar and HALO in-situ data. In particular, the difference in w is 0.0 ± 0.2 m s^{-1} on average. In the end, the given standard deviation accounts for these uncertainties in the MF profile being a worst case estimate with sub-legs included which have lengths shorter than λ_{MAX} /2 with theoretically λ_{MAX} ≈ 700 km. The fact that the mean MF profile computed from the set of sub-legs is close to the MF profile averaged for the full leg distance [-300, 400 km], which has the largest likelihood to capture the full wave cycles of the wave packages, supports that the sub-legs are chosen in a proper way (new Fig. 16).

additional reference:

Brown, P. R. A.: Aircraft measurements of mountain waves and their associated momentum flux over the British Isles, Quarterly Journal of the Royal Meteorological Society, 109, 849–865, https://doi.org/10.1002/qj.49710946211, https://rmets.onlinelibrary.wiley.com/doi/abs/10.1002/qj.49710946211, 1983.

+Measurements vs realistic simulations: The wave field is much more complicated and complex compared to the idealized boundary layer case. The MF profiles can be distinguished for the three wave classes defined above. The most prominent feature is the kink reaching positive values for the long waves between 8-km and 9-km altitude. Negative fluxes of the same magnitude are found below. The mean MF at 7.8-km altitude of the DWL and the HALO in-situ data differs but within the range of the uncertainty. It is worth mentioning that the uncertainty in the MF from the in-situ data is largest at this altitude and larger than the uncertainty derived for the DWL data. This means the MF from in-situ at this altitude could be biased to MF of larger magnitude due to localized peaks in ρu'w' along the leg. The intermediate and short scale waves show similar MF profiles with small undulations around zero. The leg-averaged momentum flux of the long waves is positive (around −0.05 Pa) at 13.3-km altitude which could be a hint for wave reflection in the stratosphere or a stratospheric source creating downward propagating GWs.

For the simulations, the MF profiles of the three wave classes clearly distinguish from each other (Fig. 16). The pronounced kink in the MF profiles of the long waves (>30 km) and the short waves (<10km) in the altitude range of 7 km to 9 km is a clear feature of the effect of the TIL and not visible in the no-TIL simulation (Fig. 16a). The amplitudes of the long (i.e. mountain waves) and intermediate waves (i.e. reflected and trapped waves in the troposphere) and their resulting MF are overestimated compared to the observations (Fig. 6 and Fig. 15f-i). The MF is overall negative for these simulations but close to zero for the short waves. These findings are most likely an effect of the 2-dimensional model setup. Interestingly, the MF of the long waves shows a larger magnitude in the simulation without TIL (Fig. 16a) compared to the simulation with TIL (Fig. 16b). The MF of the intermediate waves shows an opposite behavior, i.e. smaller in magnitude in the simulation without TIL. This change in MF between the two simulations suggests stronger reflection of the MWs at the TIL. This is a finding that is in agreement with findings from the single mountain simulations.

Summary:

This article presents an interesting observed case of trapped mountain waves that suggests the importance of interfacial dynamics along a tropopause inversion layer (TIL). The observations are unique and make the article a valuable contribution from the observational analysis alone. The study is further enhanced by interesting sensitivity studies using a 2D model comparing the wave response in both boundary layer inversion and TIL scenarios. I strongly recommend that the analysis done for Figure 13 be expanded to include the TIL simulation (see below). But overall the simulations represent a compelling initial investigation into this mechanism not previously observed in the UTLS. Although the simulations lead to further questions, I agree that further investigation is appropriately left to future studies. The article is generally well-written, although a few points that should be rewritten (particularly in the Introduction) are highlighted below.

We thank the reviewer for this positive feedback and his/her valuable suggestions that helped to improve the manuscript. We revised and shortened the introduction as suggested. As already described above, we also revised the MF analysis and determined MF profiles for the no-TIL/TIL simulation with realistic topography.

Specific comments:

paragraph starting at line 30: what is the point of this paragraph? I think you are trying to give an overview of our understanding of gravity wave propagation from the troposphere to the upper atmosphere, but you include a lot of older work just to say that it's more complicated than basic theory. That is not a new finding. The sentence at line 41 starting "Fine scale structures…" is directly relevant to your work. But the rest of the paragraph can be condensed/cut.

If you choose to keep more of the background information, several sentences are awkwardly worded or confusing and should be fixed:
1. line 40: “This makes the wave spectrum (i.e. wavelengths) being determined by the vertical varying wind and stability and not by the topography spectrum which affects the relative amplitudes”: confusing sentence. Do you mean: “In other words, the wave spectrum (i.e. wavelengths) and wave amplitudes are determined by the vertical varying wind and stability and not by the topography spectrum.”
We decided to keep some of the background information for completeness but shortened the paragraph and revised the wording.
…

Vadas et al., 2003). GWs are propagating from their sources in the troposphere and the tropopause region (Sato et al., 2009; Fritts et al., 2016). However, the atmospheric temperature and wind structures influence the propagation of GWs and alter their properties.

Starting with the work of Queney (1948) and Scorer (1949), mountain wave (MW) propagation in the atmosphere was intensively investigated using theoretical and numerical methods. An important and well known result of these investigations is that the stratospheric solution in a model taking into account a vertically varying background is not dominated by the classical solution of Queney (1948) but by reflected and downstream propagating (trapped) waves in the troposphere (Wurtele et al., 1987; Keller, 1994). The wave spectrum (i.e. wavelengths) is determined by the vertical varying wind and stability and not by the topography spectrum. The topography affects the relative amplitudes (Keller, 1994; Ralph et al., 1997). Fine scale structures in the atmosphere, such as sharp temperature inversions at the top of the boundary layer (Vosper, 2004; Sachsperger

…

2. lines 44-46: These two sentences are awkwardly stated and I’m not sure why they’re needed.
We added a reference to mountain wave drag parametrizations to highlight that the hydrostatic approximation is still of importance nowadays.
…
Linear nonrotating hydrostatic wave theory is most commonly used by mountain wave parameterizations in weather and climate models to propagate these waves away from the subgrid-scale orography to higher levels (Eckermann et al., 2015).

line 82: a “tight” discussion? What do you mean by “tight” in this context?
We revised the sentence.
…
The results are discussed in Section 4 and Section 5 concludes the paper.

line 118: need to state what alpha represents
The sign was the “proportional to” sign. To avoid this misunderstanding we now give the exact definition.
…
leg-averaged momentum flux ($\mathrm{MF} = \overline{\rho}\overline{u'w'}$)

Figure 6: Interesting figure, but the caption was hard to follow. A few rewrite suggestions: “Black contour lines mark regions significant at the 95%-confidence level. The cone of influence is shaded in grey. Flight legs located below the tropopause (see labelled mean flight altitudes) are marked with grey background colour.”
-also Figure 6: Is the black dashed line showing the thermal tropopause location?

We clarified the caption as suggested. The black dashed line marks the 10-km horizontal wavelength.

Figure 6. Cross mountain flight legs of Falcon and HALO for (a) in-situ vertical wind and topography and (b) corresponding wavelets with the horizontal wavelength given on the y-axis. The dashed horizonal line marks 10-km horizontal wavelength that separates short and intermediate scale waves. Black contour lines mark regions significant at the 95%-confidence level. The cone of influence is shaded in grey. Flight legs located below the tropopause (see labelled mean flight altitudes) are marked with grey background colour. Time t_0 indicates when the aircraft was located at X_0 (see Fig. 1) and shows that PGS11 HL1 and RF08 FL1 (labelled with yellow boxes) took place nearly at the same time (HALO was flying 30 seconds behind Falcon).

line 238: “and a free slip lower boundary condition is used.”
Done, we changed the sentence as suggested.

line 247: “The signal downstream of the terrain is”
Done, we changed the sentence as suggested.

Figure 13: This is a compelling figure for the boundary layer inversion (RUN 2) interfacial wave analysis, but why is this same analysis not shown for the TIL (RUN 4)? An additional panel would strengthen your argument.
As described above, we revised the MF analysis. Instead of showing the MF analysis for RUN 4 (which is in the Bousinesq framework), we did the analysis for RUNs 5 and 6. We added the MF profiles for these no-TIL/TIL simulation with realistic topography in new Fig. 16.
…
The pronounced kink in the MF profiles of the long waves (>30 km) and the short waves (<10km) in the altitude range of 7 km to 9 km is a clear feature of the effect of the TIL and not visible in the no-TIL simulation (Fig. 16a).
…

Modified and new figures

- modified (new aspect ratio):

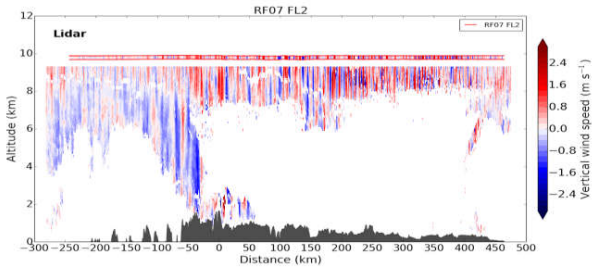

Figure 8. Vertical winds along flight leg RF07 FL2 measured by the DWL and in-situ instruments (marked by red horizontal lines) at flight level by the DLR Falcon.

- modified (new aspect ratio):

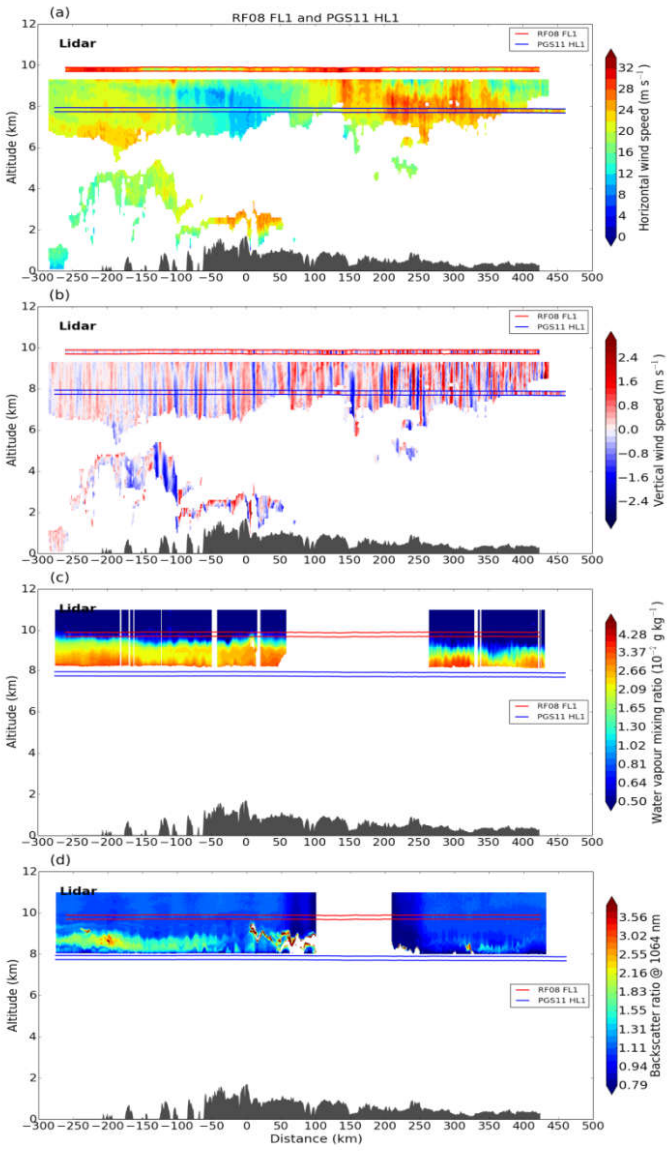

Figure 9. DWL measurements of (a) horizontal wind speed and (b) vertical wind speed and WALES measurements of (c) water vapour mixing ratio and (d) lidar reflectivity along flight leg RF08 FL1/PGS11 HL1 combined with corresponding in-situ measurements of HALO and DLR Falcon at flight level (marked by blue and red horizontal lines).

- modified (revised data analysis):

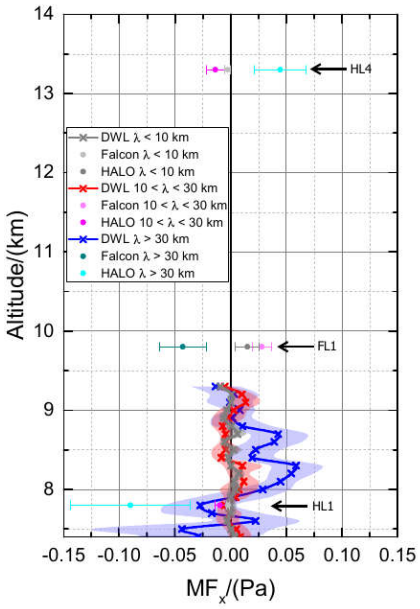

Figure 10. Leg-averaged momentum fluxes as mean for varying leg length (solid) with standard deviation (shading, error bars) along flight leg RF08 FL1 obtained from DWL (×) and in-situ measurements (●) which include also PGS11 HL1 and HL4. Three wave classes are colour coded and bold black line separates positive and negative fluxes.

- modified (additional panels):

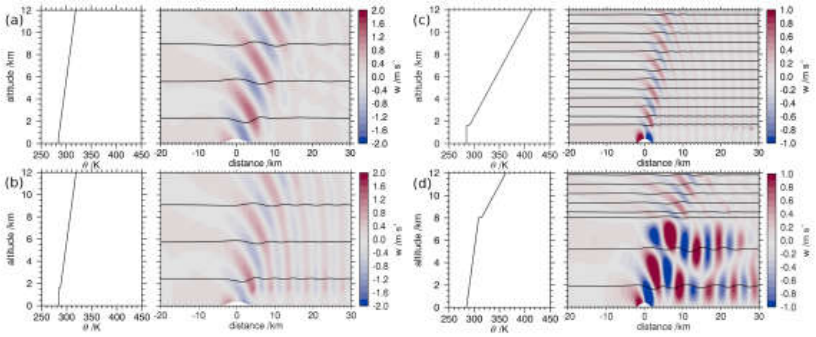

Figure 11. Potential temperature and vertical velocity of the idealized simulations of the cases with (a) a neutral boundary layer without inversion and $N_U = 0.01\ \mathrm{s}^{-1}$ (RUN 1), (b) a neutral boundary layer with an inversion of 3.3 K and $N_U = 0.01\ \mathrm{s}^{-1}$ (RUN 2), (c) a neutral boundary layer with an inversion of 6.6 K and $N_U = 0.02\ \mathrm{s}^{-1}$ (RUN 3), and (d) a stable troposphere ($N = 0.01\ \mathrm{s}^{-1}$) with a TIL of 6.6 K and $N_U = 0.02\ \mathrm{s}^{-1}$ (RUN 4).

- modified (revised data analysis, new panels):

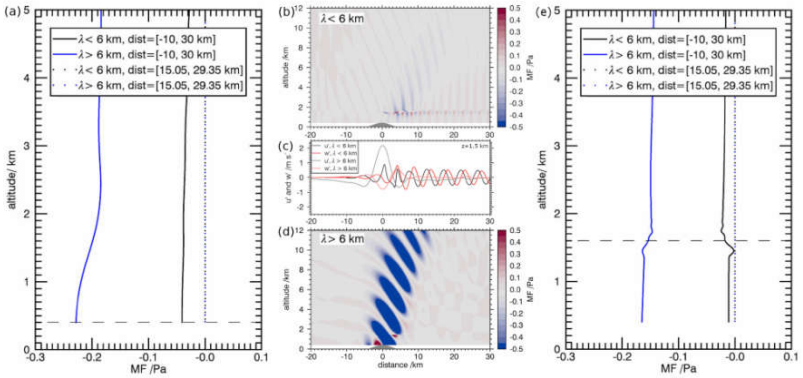

Figure 13. Momentum flux (profiles) for (a) RUN 1 without boundary layer inversion (Figs. 11a, 12a) and (b,d,e) Run 2 with boundary layer inversion (Figs. 11b, 12c) for two wave classes (horizontal wavelength smaller or larger 6 km). Profiles show averages for the full distance (solid) and for the downstream distance (dotted); horizontal dashed lines marks the top of the boundary layer. (c) shows u' and w' for the two wave classes at 1.5 km altitude revealing their phase relationship right below the inversion, i.e.- 90° for interfacial waves (black and red lines).

- modified (new aspect ratio):

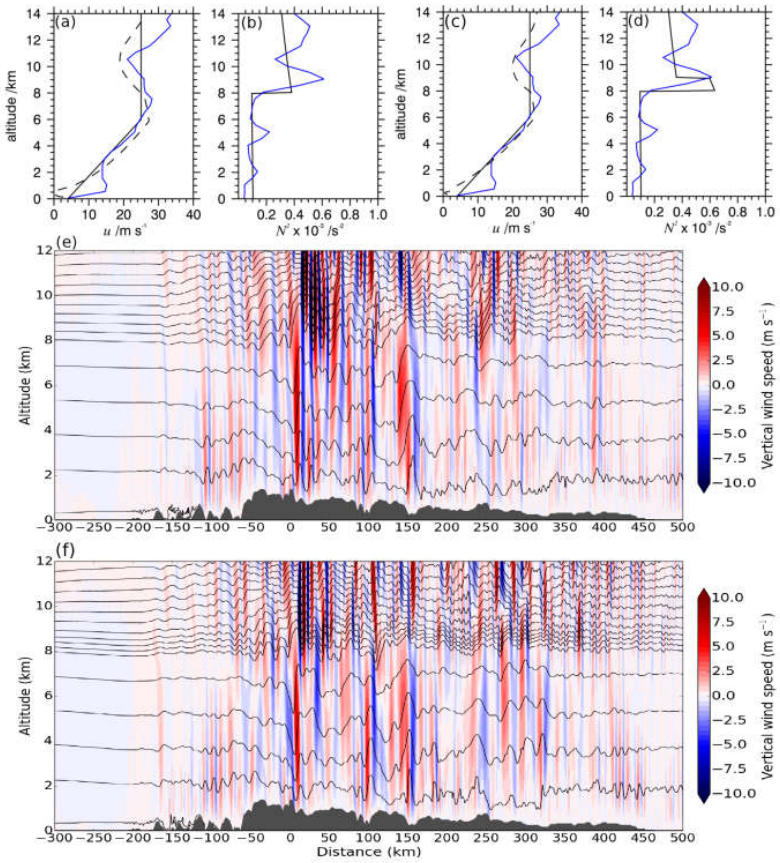

Figure 14. Initial profiles (black solid) and vertical velocity for the simulations with more realistic terrain without TIL (a, b, e; RUN 5) and with TIL (c, d, f; RUN 6). The initial profiles approximate the background conditions over southern Scandinavia on 28 January 2016 (blue profiles show the Stavanger radiosonde data). Negative shear above the tropopause establishes in the course of the simulations (a, d; black dashed, time = 16 h, distance = −150 km).

- new figure:

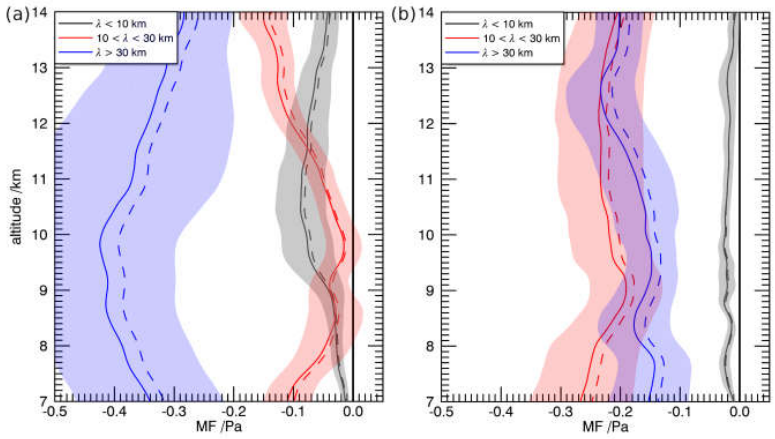

Figure 16. Averaged momentum fluxes for (a) RUN 5 (no TIL) and (b) RUN 6 (TIL) as mean for varying leg length (solid) with standard deviation (shading) and for the full leg distance [-300, 400 km] (dashed). Three wave classes are color coded and bold black line separates positive and negative fluxes